Optics & Laser Technology 44 (2012) 1393–1397

Contents lists available at SciVerse ScienceDirect

Optics & Laser Technology

journal homepage: www.elsevier.com/locate/optlastec

Integrated interferometer for monitoring three-dimensional vibrations by discrete aperture

Xuejie Zhang*, Wei Huang, Dean Liu, Tao Feng, Yan Zhang, Pingping Sun, Jianqiang Zhu

Shanghai Institute of Optics and Fine Mechanics, Chinese Academy of Sciences, P.O. Box 800-211, Shanghai 201800, China

ARTICLE INFO

Article history:
Received 7 June 2011
Received in revised form
6 November 2011
Accepted 12 December 2011
Available online 16 January 2012

Keywords:
Vibration measurement
Interferometer
Three-dimension

ABSTRACT

This paper presents a new method for measuring vibration based on interference from two spherical waves. By integrating the two interference arms into a beamsplitter cube by reflective film and dividing the probe beam into two parts with discrete apertures, the interferometer can distinguish that the vibrations are from the monitored optical components or from laser interferometer system itself. At the same time, because the two interference waves are spherical, it can realize monitoring the three-dimensional vibrations. The measurement system has advantages of being stable and reliable with an integrated structure. Theoretical analysis and experimental demonstration are performed. The experiment results indicate that the method can monitor three-dimensional vibrations accurately.

1. Introduction

High power laser system, such as the National Ignition Facility, which always has hundreds of optical components and long beam path, is very sensitive to any vibration in laser chain [1]. Because the vibrations can cause the optical components move relative to each other and the beam deflects, it would be very important to monitor three-dimensional vibrations of optical components effectively. It is well known that the interferometry possess the highest sensitivity for measurements of some physical parameters including displacement, vibration, deformation, etc. [2–4]. Due to its high resolution, good precision and noncontact measurement, various laser interferometry techniques have been developed and used for specific purposes [5]. Interferometer has become a primary direction for investigation and is widely employed for detecting displacement and vibration at present.

There are two kinds of laser interferometers: the homodyne interferometer with a one-frequency laser [6–11] and the heterodyne interferometer with a two-frequency laser [12–15]. Most of them use Michelson interferometer or a similar optical structure. It consists of two arms—one containing the specular test object and the other containing the reference mirror [5,16]. Reflected waves from the two arms interfere at the detection plane. The intensity of the interference signal varies depending on the optical path difference between the reference beam and the measurement beam. Therefore, the measurement parameters can be calculated by interference signal. But owing to frequency mixing, there is a first-order nonlinearity error in the heterodyne interferometer. And its nonlinearity is much larger than that of homodyne interferometer [10,15]. Another advantage of homodyne interferometer is that both resolution and accuracy are frequency independent. The upper bandwidth limit is determined by the response time of the detector and the bandwidth of signal processing electronics. With the development of interference technology, using phase-shifting and phase subdivision technology in homodyne interferometer can enhance the resolution [17,18].

However, the homodyne interferometers mostly use plane wave to measure vibrations. One of its serious drawbacks is its insensitivity to the in-plane vibration. In other words, common specular optoelectronic vibration measurement systems can only monitor vibration in one direction [6–9]. Another drawback is the changes of interference fringes, which are caused by instability of the interferometer system itself, are unavoidable. It is very difficult for conventional vibration monitoring methods to distinguish the changes of interference fringes are from the test object or from laser interferometer system itself in deed. For example, the vibration of reference mirror or the shift of frequency of laser itself can also lead to change in measurements [11].

Therefore we design a new interferometric system, which uses interference from two spherical waves to realize three-dimensional vibration measurement. And it can monitor the stability of interferometer system itself and distinguish the sources of the fringe changes by a new integrated coating design. This system is very stable and reliable.

The paper is organized as follows. Section 2 describes the proposed system and theoretical analysis. Section 3 gives the experimental device and obtained results. Finally, in Section 4, the influence of the test object vibration on interference fringes is discussed.

* Corresponding author.
E-mail address: sddxzxj@126.com (X. Zhang).

0030-3992/$ - see front matter © 2011 Elsevier Ltd. All rights reserved.
doi:10.1016/j.optlastec.2011.12.027

2. Laser interferometry system

A schematic diagram of the measurement system presented is shown in Fig. 1. The optical system is based on a beamsplitter cube of special coating design. One of the exit facets of the beam splitter is wholly coated with reflective film. Another exit facet, however, is only coated around, which leaves a hole in the center so that the optical beam can pass through. The source is a frequency stabilized He–Ne laser. After passing through an objective and a pinhole, the laser output is expanded. Then the laser beam is split into two beams by the beam splitter, a reference beam and a measurement beam. The reference beam is directly reflected by reflective film I. And the measurement beam is divided into two parts. One part around is reflected by the coating. The other part in the center is transmitted through the hole on beam splitter surface towards the test object. Then it is reflected by the cooperative target with a phase change proportional to the object's vibration. After returning to the beamsplitter cube, the measurement beam is recombined with the reference beam. And the two beams are imaged onto the sensor of a charge-coupled device (CCD) where an interference pattern is formed as a result of the interference between them. It needs to be noted that we use an objective and a pinhole in the beam path. Their main function is as a filter to enhance the interference fringe contrast. The lens L1 is mainly used to adjust the divergence of spherical wave.

Because of special coating design on the beam splitter, the interference fringes are composed of two parts, shown in Fig. 1, part A, inner interference fringes, for monitoring the vibrations from the test object, and part B, outer interference fringes, for monitoring the stability of interferometer system itself. Only in the case that part B is stationary, the system is stable and part A can provide accurate information about the test object vibration. That is to say, it distinguishes the changes of interference fringes are from the test object or from laser interferometer system itself. Furthermore, in Fig. 1, we can add a feedback subsystem, where outer fringes B are used to quantitatively compensate for changes in inner fringes A.

As previously mentioned, the two interference beams, the reference beam and the measurement beam, are both spherical waves. Let us assume that there are two point sources O and R, as shown in Fig. 2. The spherical waves radiated by them on the CCD plane are the same as the measurement wave and the reference wave on it. Therefore, the interference pattern can be considered to be formed by the two point sources. Their position can be obtained by geometrical optics. Fig. 2 shows the theoretical model of this interferometer system.

Suppose that (x_o,y_o,z_o) and (x_R,y_R,z_R) are the coordinates of point sources O and R in Fig. 2, respectively. Their phases at the pixel (x,y) on the sensor plane $z=0$ are expressed as follows:

$$\varphi_R = \frac{2\pi}{\lambda}\left\{\frac{1}{2l_R}\left[x^2+y^2-2(xx_R+yy_R)\right]+l_R\right\} \tag{1}$$

$$\varphi_o = \frac{2\pi}{\lambda}\left\{\frac{1}{2l_o}\left[x^2+y^2-2(xx_o+yy_o)\right]+l_o\right\} \tag{2}$$

where $l_R=(x_R^2+y_R^2+z_R^2)^{1/2}$, $l_o=(x_o^2+y_o^2+z_o^2)^{1/2}$, the R subscript corresponds to the reference wave, the O subscript corresponds to the object wave, and λ is the wavelength of the laser used.

As we all know, the intensity $I(x,y)$ of interference fringes reaches the maximum when the optical path difference $\Delta(x,y)$ satisfies this condition $\Delta(x,y)=n\lambda,(n=0,\pm1,\pm2,\ldots)$. So the equation about fringes position can be determined in a first approximation:

$$x^2+y^2-2x\frac{l_Rx_o-l_ox_R}{l_R-l_o}-2y\frac{l_Ry_o-l_oy_R}{l_R-l_o}-2n\lambda\frac{l_ol_R}{l_R-l_o}-2l_ol_R=0 \tag{3}$$

From (3) it is clear that the interference fringes are a series of concentric circles. The center of concentric circles is at the position (x',y'):

$$x'=\frac{l_Rx_o-l_ox_R}{l_R-l_o} \quad y'=\frac{l_Ry_o-l_oy_R}{l_R-l_o} \tag{4}$$

And on the plane $z=0$, the intensity $I(0,0)$ at the pixel (0,0) can be expressed as

$$I(0,0)=I_o\{1+\cos[2\pi(l_o-l_R)/\lambda]\} \tag{5}$$

No matter, which direction the monitored object vibrates along, the object wave returning to the CCD plane will change, that is, the position of virtual point source O will change. According to Eqs. (4) and (5), the center position (x',y') and the

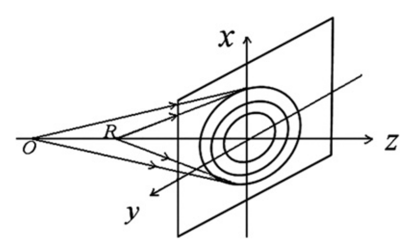

Fig. 2. Theoretical model of laser interferometer system. O: the point source corresponding to object wave; R: the point source corresponding to reference wave.

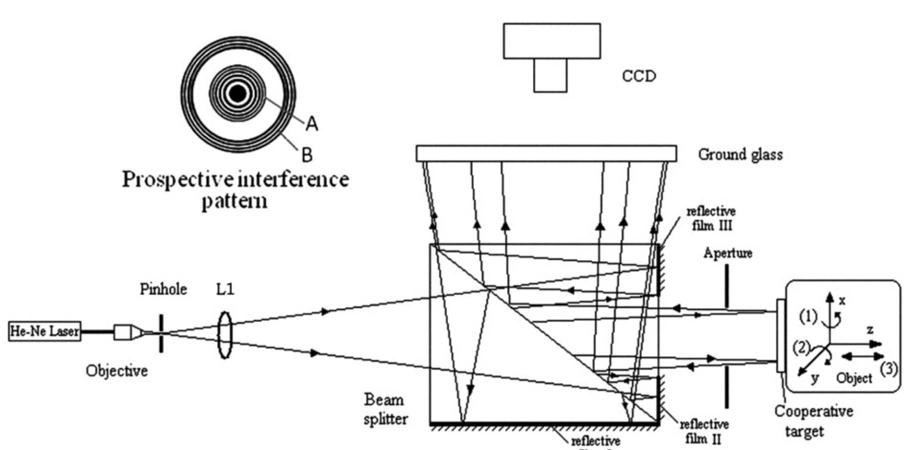

Fig. 1. Schematic diagram of integrated interferometer. L1: lens.

intensity $I(0,0)$ will vary with (x_o,y_o,z_o). By measuring the three variables, we can calculate the vibration parameters of the test object. So the interferometer system can realize three-dimensional vibrations measurement.

When x_o,y_o and z_o vibrate simultaneously, the interference fringes will contract or expand, meanwhile, the center position will change. Since the reference wave is constant, make the coordinate of the point sources R as $(0,0,z_R)$. Suppose the initial coordinate of the point sources O is $(0,0,z_{o1})$ and the vibrations in three directions are $\Delta x_o,\Delta y_o$ and Δz_o, respectively.

From Eq. (5), $I(0,0)$ shows sinusoidal variation with a cycle of λ. Each time l_o has a change of λ, $I(0,0)$ will change from bright to dark once. So the change of l_o can be obtained by $I(0,0)$. Due to $z_{o1} \gg \Delta x_o,\Delta y_o$, the vibration Δz_o can be considered equal to the change of l_o. And the direction of the vibration Δz_o can be obtained by interference fringes contraction or expansion. The measurement in z direction can reach at least a resolution of $\lambda/2$.

Due to $z_{o1} \gg \Delta z_o,\Delta x_o,\Delta y_o$, Eq. (4) can be converted to $\Delta x_o=(1-z_{o1}/z_R)x'$ and $\Delta y_o=(1-z_{o1}/z_R)y'$. The vibrations Δx_o and Δy_o can be obtained by changes of center position (x',y'). Their resolution, which is affected by the CCD resolution and the ratio of z_{o1} to z_R, can reach 0.1 μm. The corresponding measurement range is ± 50 μm. The appropriate resolution and measurement range can be selected by adjusting the ratio of z_{o1} to z_R during the measurement. It can be achieved by adjusting the lens L1in Fig. 1.

Through the above analysis, it is concluded that no matter, which coordinate component of the virtual point source (x_o,y_o,z_o) vibrates, the system is detectable. So the interferometer system can realize monitoring three-dimensional vibrations.

In the proposed system, a plane mirror is used as the cooperative target to combine with the test object, for measuring vibrations in the rotation directions around x-axis and y-axis and vibrations in the translation direction along z-axis, shown by the arrows in Fig. 1. If we want to measure vibrations along x-axis or y-axis, a spherical mirror can be used as cooperative target instead of the plane mirror. The principle is the same as above. In this paper, we only discuss the former.

3. Experiments and results

The experimental setup is similar with Fig. 1. Because we just want to test the principle of this method, the experimental device adopted here is slightly different from the configuration described above. We used a mirror (50 mm from the splitter) instead of the reflective film I and inserted two mirrors between the beamsplitter and the object instead of reflective film II and III. The test object was a mirror (100 mm from the splitter). And the image plane was a white card with a coordinate system (2.4 m from the splitter). The interference patterns were recorded with a camera.

Here, we used lens L1 of focal length $f=150$ mm, located 135 mm from the pinhole. Based on object–image formula, the image distance is 1350 mm. Combined with the distance between L1 and the splitter (99.2 mm), the position of the two virtual point sources can be calculated. In the initial state, coordinates of the point sources corresponding to the reference wave and the measurement wave were (0,0,4) and (0,0,4.1) (unit: m), respectively. Fig. 3 shows the interference pattern formed in initial state. It is clear that the interference pattern is basically the same as what is expected. The fringes in the middle correspond to the measurement wave reflected by the test mirror. The ones on both sides correspond to the wave reflected by the two inserted mirrors and they are used as a judgment of the reliability of this system. So these two parts can be used to monitor the vibrations from the test mirror and interferometer system itself.

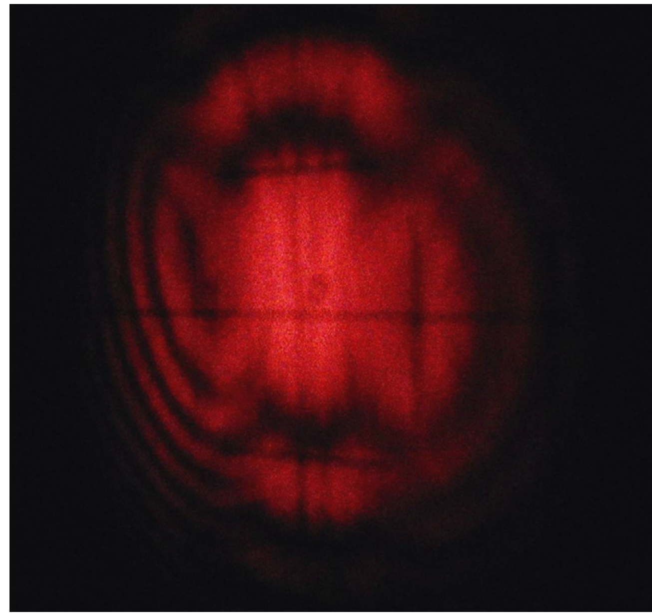

Fig. 3. Interference pattern in the initial state.

First, make x_o vibrate between -0.8 mm and 0.8 mm, y_o and z_o remain unchanged. We took 9 interference patterns in steps of 0.2 mm and they were numbered as shown in Fig. 4(a). During the measurement, we found basically no changes in the fringes on both sides. It means the system was stable and the results were available. By comparing the interference patterns listed in Fig. 4(a), it is found the vertical coordinate x' of the center changes with x_o, whereas the horizontal coordinate y' remains basically unchanged. The relationship between them will be described in detail in next section. Similarly, when only y_o vibrated, the interference patterns are shown in Fig. 4(b).

In order to observe the influence of Δz_o on interference fringes, we removed the two inserted mirrors, and only used the reference mirror and the test mirror. During the vibration of z_o, we observed the phenomenon of the interference fringes contraction and expansion. Meanwhile, the center fringe showed periodical variation from bright to dark. We chose two interference patterns in different states (shown in Fig. 5) to show the fringes' periodical variation in this experiment. One's center fringe is dark, and the other's is bright.

Because of the limitation of experimental condition and equipments, the experiment results are not in high precision. And it is not very ideal in monitoring the vibrations from interferometer system itself, due to the beamsplitter cube not coated and the structure not integrated. Nevertheless, these experiment results can still show that this method can effectively monitor three-dimensional vibrations.

4. Discussion

The theory and experimental setup of the proposed method have been described above. It is very important for us to know the vibration characteristics from interference patterns. In the initial state, coordinates of the point sources corresponding to the reference wave and the measurement wave are (0,0,4) and (0,0,4.1), respectively.

When only x_o vibrates, substituting these data into Eq. (4), it can be derived that $y'=0$ and $x'=-40\Delta x_o$, where l_o is thought to be constant. It is consistent with the experiment result that y'

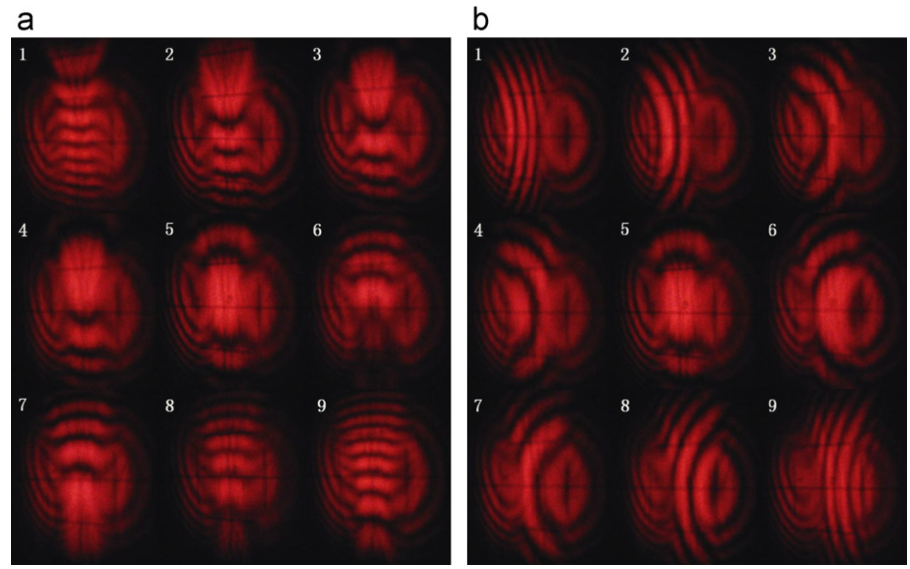

Fig. 4. Interference patterns (a) obtained in steps of 0.2 mm when x_o vibrated from -0.8 mm to 0.8 mm. (b) obtained in steps of 0.2 mm when y_o vibrated from -0.8 mm to 0.8 mm. Scale span: 1.5 cm.

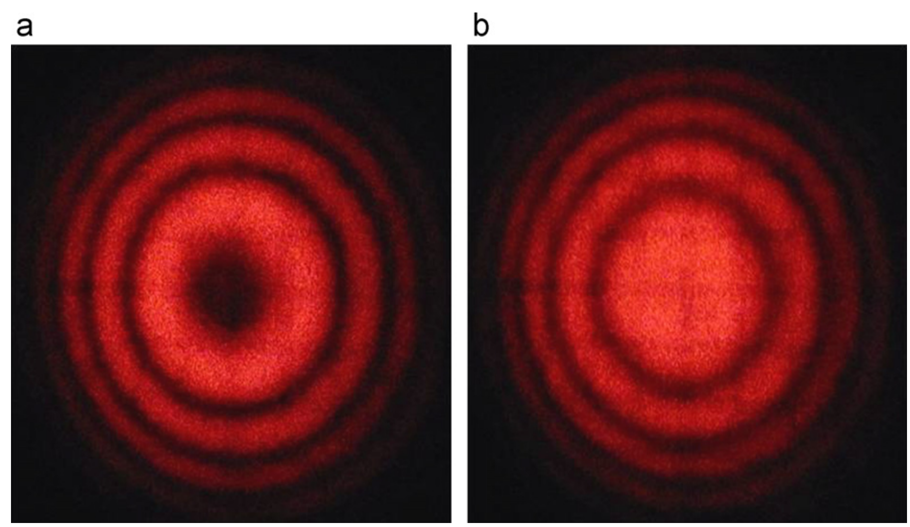

Fig. 5. Two interference patterns obtained when z_o vibrated.

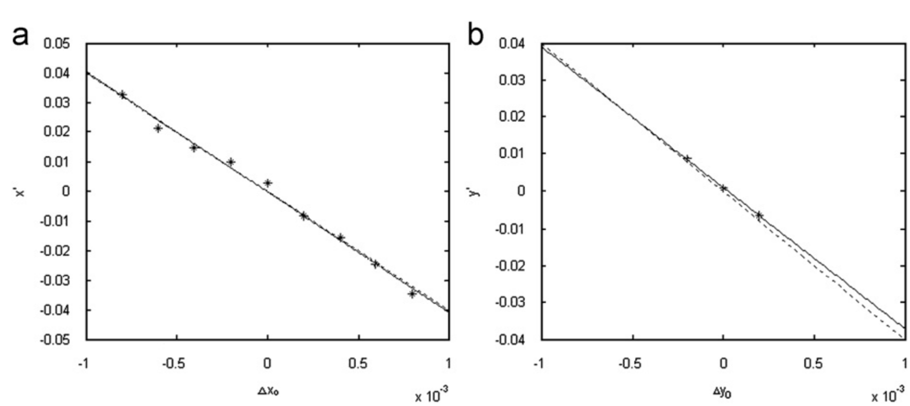

Fig. 6. (a) The relationship between x' and Δx_o and (b) the relationship between y' and Δy_o. The dashed lines: theoretical curves; the solid lines: experimental curves.

remains basically unchanged. And there is a linear proportion by inversion between x' and Δx_o, as shown in Fig. 6(a) by the dashed line. For comparison, the corresponding actual curve, which is obtained through the experimental results in Section 3, is given by the solid line in Fig. 6(a). Its fitting equation is $x' = -40.286\Delta x_o$, and the error is 0.715%.

The relationship between y' and Δy_o is obtained using a similar procedure, shown in Fig. 6(b). Owing to the limitations of experiment equipments, we only obtain Y-coordinate y' of center from three interference patterns (serial number: 4, 5, 6) in Fig. 4(b). So there are only three points in Fig. 6(b) (the fitting equation is $y' = -40.55\Delta y_o + 0.0002$). But on the whole, the experimental curves and theoretical curves agree well. If the imaging system is a CCD, measurement precision and resolution both can be further improved, and vibration frequency can also be obtained. The above analysis shows that the method proposed here can measure vibrations accurately.

5. Conclusion

We have proposed a new interferometric method for measuring three-dimensional vibrations. The design of discrete apertures can be used to monitor the stability of interferometer system itself and distinguish the vibration sources. Experiments for principle demonstration were carried out. We observed the changes of interference fringes induced by vibrations in three directions. The vibration parameters can be obtained by measuring the intensity $I(0,0)$ and the variation of center position. If the interferometer is integrated into a compact structure and a CCD is used, the contrast ratio of interference fringes and experimental results will be better than shown in this paper, and the practical precision of this method should be analyzed further.

References

[1] Trummer DJ, Foley RJ, Shaw GS. Stability of optical elements in the nif target area building. Proceedings of the SPIE 1999;3492:363–71.
[2] Pan WY, Cross LE. A sensitive double beam laser interferometer for studying high frequency piezoelectric and electrostrictive strains. Review of Scientific Instruments 1989;60:2701–5.
[3] Bobroff N. Recent advances in displacement measuring interferometry. Measurement Science and Technology 1993;4:907–26.
[4] Stepanov SI, Sokolov IA, Trofimov GS, Vlad VI, Popa D, Apostol I. Measuring vibration amplitudes in the picometer range using moving light gratings in photoconductive GaAs:Cr. Optical Letters 1990;15:1239–41.
[5] Hariharan P, Optical interferometry. 2nd ed. New York; 2003.
[6] Ngoi BKA, Venkatakrishnan K. Noncontact homodyne scanning laser vibrometer for dynamic measurement. Optical Engineering 2000;39:510–5.
[7] Suzuki T, Sasaki O, Higuchi K, Maruyama T. Real time displacement measurement in sinusoidal phase modulating interferometry. Applied Optics 1989;28:5270–4.
[8] Chao C, Wang ZH, Zhu WG, Tan OK. Scanning homodyne interferometer for characterization of piezoelectric films and microelectromechanical systems devices. Review of Scientific Instruments 2005;76:063906-1–4.
[9] Liu X, Clegg W. Polarization interferometer for measuring small displacement. Measurement Science and Technology 2001;50:868–71.
[10] Eom TB, Kim JY, Jeong K. The dynamic compensation of nonlinearity in a homodyne laser interferometer. Measurement Science and Technology 2001;12:1734–8.
[11] Liu BB, Yang J, Liu ZH, Yuan LB. Laser interferometer nanometer vibration measurement experiment based on LabVIEW workbench. Proceedings of the SPIE 2007;6830. 68301X-1-68301X-7.
[12] Sodnik Z, Fischer E, Ittner T, Tiziani HJ. Two-wavelength double heterodyne interferometry using a matched grating technique. Applied Optics 1991;30: 3139–44.
[13] Yokoyama S, Yokoyama T, Araki T. High-speed subnanometre interferometry using an improved three-mode heterodyne interferometer. Measurement Science and Technology 2005;16:1841–7.
[14] Demares FC. High-resolution, high-speed, low data age uncertainty, heterodyne displacEment measuring interferometer electronics. Measurement Science and Technology 1998;9:1024–30.
[15] Hou W. Optical parts and the nonlinearity in heterodyne interferometers. Precision Engineering 2006;30:337–46.
[16] Born M, Wolf E, Principles of optics. 7th ed. New York; 1999.
[17] Bitou Y. Closed-loop phase-shifting homodyne interferometry using heterodyne phase detection. Applied Optics 2008;47:6219–25.
[18] Pisani M. A homodyne Michelson interferometer with sub-picometer resolution. Measurement Science and Technology 2009;20:084008.